RSC Advances

ROYAL SOCIETY OF CHEMISTRY

www.rsc.org/advances

"For Table of Contents Use Only"

Effect of fluorination on the performance of poly(thieno[2,3-*f*]benzofuran-*co*-benzothiadiazole) derivatives

Ruili Cui [a#] Ling Fan [a #] Jun Yuan [a] Lihui Jiang [a] Guohui Chen [a] Yanhuai Ding [b] Ping Shen [c] Yongfang Li [d] Yingping Zou [a*]

Three polymers named PTBFBT-0F, PTBFBT-1F, PTBFBT-2F were synthesized, the effects of different fluorine numbers on donor-acceptor conjugated polymers in photophysics and photovoltaic properties were thoroughly investigated. PCE of 5% with PTBFBT-2F as the donor was obtained.

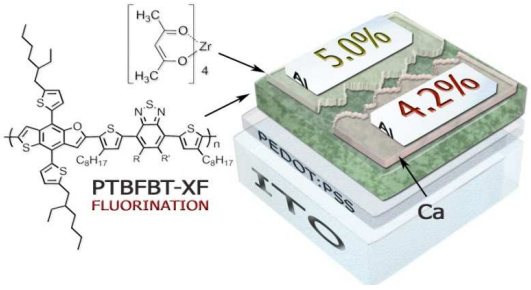

Cite this: DOI: 10.1039/c0xx00000x

www.rsc.org/xxxxxx

ARTICLE TYPE

Effect of fluorination on the performance of poly(thieno[2,3-*f*]benzofuran-*co*-benzothiadiazole) derivatives

Ruili Cui [a#] Ling Fan [a #] Jun Yuan [a] Lihui Jiang [a] Guohui Chen [a] Yanhuai Ding [b] Ping Shen [c] Yongfang Li [d] Yingping Zou [a*]

Received (in XXX, XXX) Xth XXXXXXXXX 20XX, Accepted Xth XXXXXXXXX 20XX

DOI: 10.1039/b000000x

In order to shed light on the effects of different fluorine numbers on donor-acceptor (D-A) conjugated polymers in photophysics and photovoltaic properties, three polymers named PTBFBT-0F, PTBFBT-1F, PTBFBT-2F were synthesized and thoroughly investigated. The nonfluorinated benzothiadiazole (BT) polymer (PTBFBT-0F) has a highest occupied molecular orbital (HOMO) energy level of -4.98 eV and a low bandgap of 1.64 eV. When one of the hydrogen atom of BT unit was substituted by fluorine atom (PTBFBT-1F), a little blue-shift UV-Vis absorption and a lower HOMO energy level of -5.11 eV, thus a similar V_{oc} and J_{sc} were obtained. Nevertheless, the *FF* of PTBFBT-2F was further improved from 46% to 53% due to the relatively higher and balanced electron/hole charge transport mobility of 1.83×10^{-5} $cm^2\cdot v^{-1}\cdot s^{-1}$ and 1.52×10^{-5} $cm^2\cdot v^{-1}\cdot s^{-1}$. Using a Ca/Al top electrode, devices based on PTBFBT-0F, PTBFBT-1F, PTBFBT-2F as electron donor showed the increasing power conversion efficiency (PCE) of 3.0%, 3.6% and 4.2%, respectively. Furthermore, replacing Ca with zirconium acetylacetonate film (ZrAcac) as cathode buffer layer (CBL), PCE of 5% with PTBFBT-2F as the donor was obtained.

Introduction

Bulk heterojunction (BHJ) polymer solar cells (PSCs) sandwiched a blend layer of conjugated polymer donor and fullerene derivative acceptor between a transparent ITO positive electrode and a low work function metal negative electrode. Since the BHJ PSC was reported in 1995,[1] the PCE of the PSCs has been improved gradually by designing new donor and acceptor materials as well as new device structures, and recently the PCE has exceeded 10%.[2-6] Although high PCE was obtained, the efficiency and stability are still needed to get enhancement towards realizing commercialization. Thereby, researches on device structures tend to focus on conventional devices, tandem configurations[4, 7] and inverted devices.[8-10, 11, 12] Development on new

photovoltaic materials has mainly focused on creating new donor-accepter (D-A) conjugated polymers with alternating electron-rich and electron-deficient units along the polymer main chain, because their bandgap and energy levels can be easily tuned by controlling the intramolecular charge transfer (ICT) from the D unit to the A unit.[13] In order to obtain higher PCE, donor materials with improving charge transporting properties, narrowing the band gap (E_g), deeper HOMO energy levels and superior solubility as well as miscibility with fullerenes are urgently needed. Because these parameters are traded-off, it is a great challenge to design and synthesize a material to meet all these requirements.

From the previous work, the F atom has many merits for improving the photovoltaic performance, for example, (a) the strong electronegativity induces greater intramolecular and intermolecular interactions which can optimize the morphology of the active layer;[14-16] (b) the strong electron-withdrawing nature that can lower the HOMO energy level, thereby increase the V_{oc} of PSCs;[17, 18] (c) the induced dipole may also facilitate charge transfer with less geminate recombination by reducing columbic interaction between electron and hole.[19, 20] However, effect of the number of substituted fluorine atoms on PCE is rarely reported.

BT unit has been very popular in the design of photovoltaic materials due to its excellent optical and electrochemical properties. The synthesis of a conjugated polymer with a fluorinated BT unit was first reported by You *et al*., its improved performance was demonstrated compared to the unsubstituted BT moiety.[21] Other groups have subsequently reported the use of the fluorinated BT unit which in general resulted in an improved photovoltaic performance.[22-26] Therefore, the fluorinated BT unit has great potential as electron accepting unit to constructing high efficiency donor materials. Meanwhile, it is also in urgent need to find suitable donor unit. Our previous materials based on thieno[2,3-*f*]benzofuran (TBF) unit have shown an efficient PCE up to 6.4%.[27] Herein, in order to explore the effects of different F numbers on BT unit, we chose D-A polymer backbone based on TBF as the donor unit and different fluorinated BT as acceptor unit with thiophene as a π bridge.[18, 28] Accordingly, three D–A polymers, named PTBFBT-0F, PTBFBT-1F and PTBFBT-2F were designed and synthesized (scheme 1). We expect to explore the changes of V_{oc}, *FF* and J_{sc} of the mentioned polymer due to the introduction of one or two F atoms. After one fluorine atom was introduced onto the BT unit, the copolymer exhibited low-lying HOMO energy level and a little blue-shift in the UV-Vis absorption resulting in higher V_{oc} (from 0.63 V to 0.77 V) and lower J_{sc} (from 11.18 mA/cm^{-2} to 10.28 mA/cm^{-2}) as compared with those of the non-fluorinated analogue. At the same time, the *FF* was improved from 43% to 46%. Upon the introduction of the second fluorine atom onto BT,

the *FF* was further improved from 46% to 53% due to relatively higher and balanced electron/hole charge transport mobility, but almost constant J_{sc} (from 10.28 mA/cm^{-2} to 10.54 mA/cm^{-2}) and V_{oc} (from 0.77 V to 0.75 V) were obtained resulting from the similar HOMO level and bandgap. We also found that the electrochemical and optical properties of these polymers with $PC_{71}BM$ could be affected by fluorination of the polymer backbone. Therefore, introducing F atom with different numbers onto the acceptor unit in conjugated polymers will be a promising method to effectively tune their properties for optoelectronic applications.

Solution-processable and stable cathode buffer layer (CBL) is also important for promoting PCE.[29, 30]The addition of CBL is an effective strategy for simultaneously enhancing all device parameters.[31, 32] Tan *et al.* have demonstrated high performance PSCs by employing as-prepared zirconium acetylacetonate film (ZrAcac) as CBL.[33] Therefore we tried to replace Ca using ZrAcac as CBL and obtained an improved PCE from 4.2% to 5.0% for PTBFBT-2F.

Experimental section

Materials

2,6-Bis(trimethyltin)-4,8-bis(2'-ethylhexylthiophene)thieno[2,3-*f*]benzofuran (M1) ,[27] 4,7-Bis(5-bromo-4-octylthiophen-2-yl)-benzo[1,2,5]thiadiazole (M2) ,[13] 4,7-Bis(5-bromo-4-octylthiophen-2-yl)-5-fluorobenzo[1,2,5]thiadiazole (M3) ,[26] 4,7-Bis(5-bromo-4-octylthiophen-2-yl)-5,6-difluorobenzo[1,2,5]thiadiazole (M4)[21] were synthesized according to the previously reported procedures. Palladium(0)tetrakis(triphenylphosphine) ($Pd(PPh_3)_4$) was purchased from Sigma-Aldrich Chemical Co., and it was used as received. Other reagents and solvents were used as received without further purification unless stated otherwise.

Characterization

^{1}H NMR spectra of the polymers were recorded using AVANCE III 500 MHz or AVANCE III 400 MHz spectrometer in Chloroform-*d* solution at 298 K with tetramethylsilane (TMS) as internal reference (0 ppm). Number-average (M_n) and weight-average (M_w) molecular weights were measured by gel permeation chromatography (GPC) analysis with polystyrene as a standard and THF (HPLC grade) as the eluent at a flow rate of 1.0 mL·min^{-1} at 35℃. Thermogravimetric Analysis (TGA) was performed on a Perkin-Elmer TGA-7 at a heating rate of 10 K·min^{-1} under nitrogen atmosphere. UV-Vis absorption spectra were taken using a Shimadzu UV-2450 spectrophotometer. For solid state measurements, polymer solution in chloroform was cast on quartzplates. Optical bandgap was calculated from the onset of the absorption band. The electrochemical cyclic voltammetry was conducted on a Zahner IM6e

Electrochemical Workstation, in a 0.1 mol·L^{-1} acetonitrile (CH_3CN) solution of tetrabutylammonium hexafluorophosphate (*n*-Bu_4NPF_6) at a scan rate of 100 mV·s^{-1} with a glassy carbon working electrode, an Ag/AgCl reference electrode and a platinum wire counter electrode. Power X-ray diffraction (XRD) measurements were carried out with 18-kW Rigaku X-ray diffraction system. The morphologies of the polymer/$PC_{71}BM$ blend films were investigated by tapping-mode with atomic force microscopy (AFM, Multimode 8 by Bruker). Transmission electron microscope (TEM) measurements were performed in a JEM-2100F.

Device fabrication

The PSCs were fabricated with a configuration of ITO/PEDOT:PSS (40 nm)/active layer/cathode. A thin layer of PEDOT:PSS (poly(3,4-ethylenedioxythiophene): poly (styrene-sulfonate)) was deposited through spin-coating on pre-cleaned ITO-coated glass with a PEDOT:PSS aqueous solution (Baytron PVP AI 4083 from H. C. Starck) at 3000 rpm and dried subsequently at 150 ºC for 15 min in air, then the device was transferred to a nitrogen glove box, where the active blend layer of the polymer and fullerene derivative was spin-coated onto the PEDOT:PSS layer. For conjugated polymer : $PC_{71}BM$ PSCs, the active layer was formed by spin coating with *ortho*-dichlorobenzene (*o*-DCB) solution containing 10 mg·mL^{-1} polymer. The ZrAcac CBL was simply prepared by spin-coating its ethanol solution (1 mg·mL^{-1}) on photoactive layer at 3000 rpm for 30 s at room temperature, no thermal annealing or any other post-treatment was performed. Finally, top electrodes were deposited in a vacuum onto the active layer .The active area of the device was 5 mm^2.

The measurements of *J–V* characteristics and *EQE*

Current density-voltage (*J–V*) characteristics of the devices were measured with a computer-controlled Keithley 236 Source Measure Unit. A Xenon lamp coupled with AM 1.5G solar spectrum filters was used as the light source. The illumination intensity of 1000 W·m^{-2} irradiation was calibrated using a standard monocrystal Si reference cell to make sure the strict light intensity. The external quantum efficiency (*EQE*) spectra were measured by Stanford Research Systems model SR830 DSP lock-in amplifier coupled with WDG3 monochromator and 500W Xenon lamp.

Synthesis of the polymers

Synthesis of PTBFBT-0F

M1 (0.2 mmol, 178 mg), M2 (0.2 mmol, 136 mg) were dissolved into toluene (10 mL) and DMF (2 mL) under a two-necked flask. The solution was flushed with argon (Ar) for 20 min, then $Pd(PPh_3)_4$ (15 mg) was added into the flask

and this mixture was flushed with Ar for another 20 min. The reaction was heated to 110 °C gradually and stirred for 24 h at this temperature under Ar. Then the reaction mixture was cooled to room temperature and poured into methanol (100 mL) slowly. The resulting precipitate was filtered through a Soxhlet thimble, which was then subjected to Soxhlet extractions with methanol, hexane and chloroform. Finally the polymer was recovered as a solid from the chloroform fraction by rotary evaporation and the dark-blue solid was obtained (156 mg, 74%). GPC: M_n= 12.3 kDa, M_w = 30.0 kDa, PDI=2.4. ^{1}H NMR (400 MHz, $CDCl_3$): δ 8.06 (br,1H), 7.74 (br, 2H), 7.54 (br, 1H), 7.50 (br, 2H), 7.29 (br, 1H), 7.02(br, 1H), 6.97 (br, 2H), 2.94 (br, 4H), 2.25 (br, 2H), 1.26-1.54 (br, 44H), 0.88-1.26 (br, 18H).

Synthesis of PTBFBT-1F

PTBFBT-1F was synthesized from M1 and M3 similarly to the synthesis of PTBFBT-0F. PTBFBT-1F was obtained as a blue solid (144 mg, 68%). GPC: M_n = 10.0 kDa, M_w =20.9 kDa, PDI=2.1. ^{1}H NMR (500 MHz, $CDCl_3$): δ 8.02 (br, 1H), 7.68 (br, 2H), 7.55 (br, 1H), 7.50 (br, 1H), 7.33 (br, 1H), 7.08 (br, 1H), 6.97 (br, 2H), 2.94 (br, 4H), 2.24 (br, 2H), 1.26-1.54 (44H, br), 0.88-1.26 (br, 18H).

Synthesis of PTBFBT-2F

PTBFBT-2F was synthesized from M1 and M4 following the synthesis of PTBFBT-0F. PTBFBT-2F was obtained as a blue solid (142 mg, 63%). GPC: M_n = 12.9 kDa, M_w = 33.5 kDa, PDI=2.6. ^{1}H NMR (400 MHz, $CDCl_3$): δ 8.06 (br, 1H), 7.75 (br, 2H,), 7.53 (br, 1H), 7.30 (br, 1H), 7.04(br, 1H), 6.99 (br, 2H), 2.93 (br, 4H), 2.23 (br, 2H), 1.26-1.54 (br, 44H), 0.88-1.26 (br, 18H).

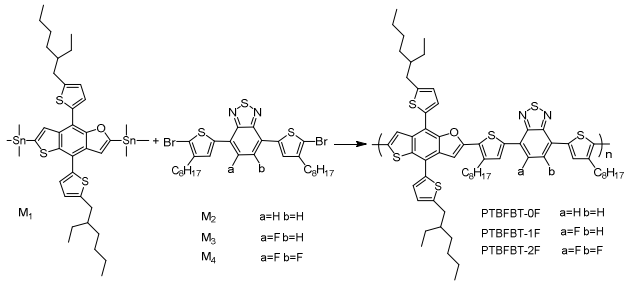

Scheme 1. Synthetic route of the polymers.

Results and discussion

Synthesis and characterization

The general synthetic route of these polymers is sketched in Scheme 1. The target polymers PTBFBT-0F, PTBFBT-1F and PTBFBT-2F were obtained through Stille coupling reactions. The synthesized polymers were purified by continuous extractions with methanol, hexane and chloroform, and the chloroform fractions were recovered. All polymers are highly soluble in common organic solvents such as chloroform, chlorobenzene and dichlorobenzene at room temperature. ^{1}H NMR spectra of the polymers are shown in Figure S1. The molecular weights of the polymers were determined by GPC using THF as eluent and polystyrene as the standard. The M_w of PTBFBT-0F, PTBFBT-1F and PTBFBT-2F is 30.0 kDa, 20.9 kDa, 33.5 kDa with polydispersity indices

(PDIs) of 2.4, 2.1 and 2.6, respectively. The related data are summarized in the Table 1.

Table 1 Polymerization results of PTBFBT-0F, PTBFBT-1F and PTBFBT-2F.

Polymer	M_n (kDa)	M_w (kDa)	PDI
PTBFBT-0F	12.3	30.0	2.4
PTBFBT-1F	10.0	20.9	2.1
PTBFBT-2F	12.9	33.5	2.6

Thermal stability

The availability of semiconducting polymers that can undertake exposure to elevated temperatures would bring a variety of new possibilities.[34] The thermal properties of PTBFBT-0F, PTBFBT-1F and PTBFBT-2F were investigated by TGA under nitrogen atmosphere, and the results are presented in Fig. 1. As we can see, all of the resulting polymers exhibited excellent thermal stability with 5% weight loss temperature of 337 ℃, 307 ℃ and 363 ℃ for PTBFBT-0F, PTBFBT-1F and PTBFBT-2F, respectively. This shows that three polymers have excellent thermal stability for device fabrication.

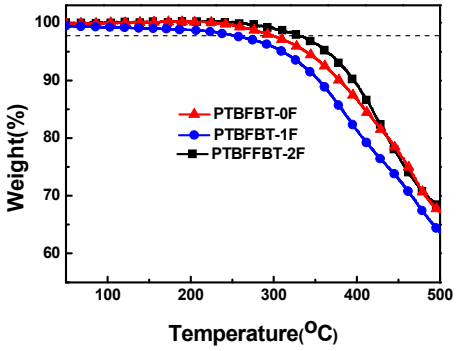

Fig. 1 TGA thermograms of these polymers with a heating rate of 10 K·min^{-1} under nitrogen atmosphere.

X-ray diffraction analysis

XRD measurement has been used to investigate the crystalline properties of conjugated polymers. Figure S2 shows the XRD patterns of the three conjugated polymers. Obviously, no peak can be found at the region from 2 to 10 degrees, indicating that no ordered laminar packing can be formed in three polymers. However, diffraction peaks around 25°, which is corresponding to the π–π stacking d-spacing of 3.56 Å, are broad and without prominent difference on intensity and location. It means that the fluorine number has little effect on the polymer chain packing structure.

Optical properties

The UV-Vis absorption spectra of these polymers in solutions and films are shown in Fig. 2, and the corresponding characteristics are summarized in Table 2. The absorption spectra of the three polymer films identically showed two major absorption peaks. One peak in the wavelength of ca. 400-500 nm is induced by the localized π–π* transition and the other is in the range of 500-700 nm originating from a typical ICT. The absorption spectra of three polymers in films are broader and red-shifted relative to those in solution. This can be ascribed to the enhanced intermolecular interactions between the polymer main chains and the planarization effect of the π-conjugated polymer backbone. In the film state, PTBFBT-1F and PTBFBT-2F have the similar onsets (λ_{onset}) and maxima (λ_{max}) values which

were blue-shifted compared with those of PTBFBT-0F. This phenomenon can be explained that the strong electron-withdrawing nature of F will increase the electron density on F atom. It leads to a permanent shift of π electron which weakened the conjugation effect resulting in blue-shifted UV-Vis absorption. Introducing F on the polymer backbone makes the λ_{onset} and λ_{max} of the polymers blue-shift which widened the energy bandgap,[17, 24, 35, 36] the corresponding data are summarized in Table 2.

Table 2 Optical and electrochemical properties of these polymers.

Polymer	Solution	Films			CV		
	λ_{max} [nm]	λ_{max} [nm]	λ_{onset} [nm]	E_g^{opt} [eV]	φ_{ox}/HOMO [V]/[eV]	φ_{red}/LUMO [V]/[eV]	E_g^{ec} [eV]
PTBFBT-0F	601	624	754	1.64	0.57/-4.98	-1.27/-3.14	1.84
PTBFBT-1F	551	601	737	1.68	0.70/-5.11	-1.26/-3.15	1.96
PTBFBT-2F	589	601	730	1.69	0.72/-5.13	-1.08/-3.33	1.80

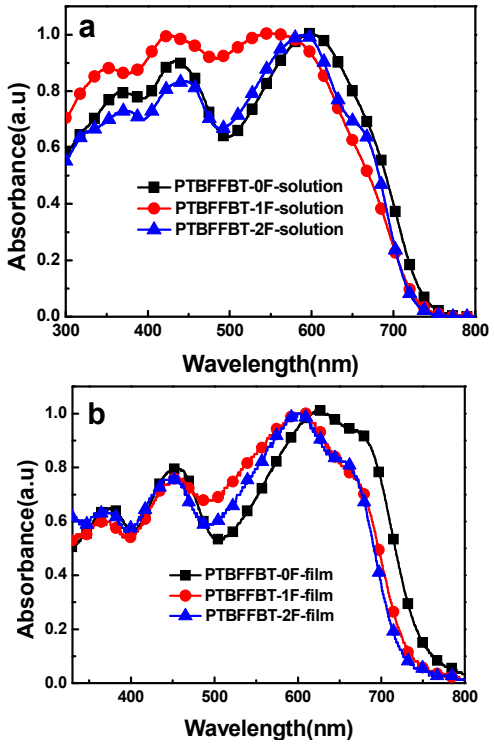

Fig. 2 UV−vis absorption spectra of polymers in chloroform solution (a) and in thin films (b).

Electrochemical properties

To determine the HOMO and lowest unoccupied molecular orbital (LUMO) levels of these polymers, cyclic voltammetry (CV) measurements were carried out under nitrogen in a three-electrode cell using 0.1M *n*-Bu_4NPF_6 in anhydrous CH_3CN as the supporting electrolyte. The CV data and curves of polymers are given in Table 2 and Fig. 3. Corresponding energy-band diagram are shown in Fig.4. HOMO and LUMO levels were determined using the equation: E_{HOMO}=-e(E_{ox}+4.41) and E_{LUMO}=-e(E_{re}+4.41).[37] The onsets of oxidation and reduction potential of PTBFBT-0F were observed at 0.57 V and −1.27 V, corresponding to HOMO and LUMO levels at −4.98 eV and −3.14 eV. For PTBFBT-1F, the onsets were observed at 0.70 V and −1.26 V, corresponding to the HOMO and LUMO levels at -5.11 eV and −3.15 eV. For PTBFBT-2F, the

onsets were observed at 0.72 V and −1.08 V, corresponding to the HOMO and LUMO levels at −5.13 eV and −3.33 eV. The electron-withdrawing nature from F atom lowers the HOMO energy level of the fluorinated polymer compared with that of the non-fluorinated analog. Muhammet E. Köse *et al* further proved it by Theoretical Calculations.[38] While there is a minor difference of the HOMO energy level between PTBFBT-1F and PTBFBT-2F. Thus, the V_{oc} of PTBFBT-1F and PTBFBT-2F are similar but higher than that of PTBFBT-0F.

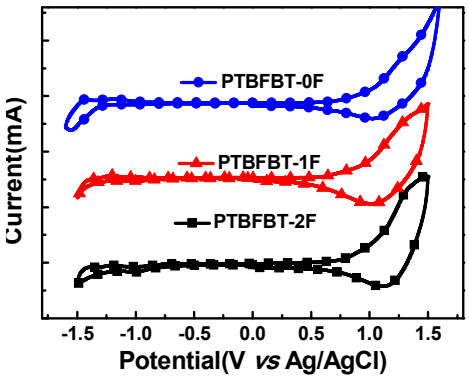

Fig. 3 Cyclic voltammograms of three polymers

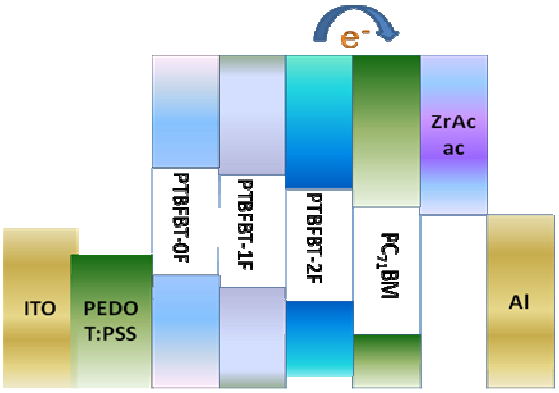

Fig. 4 Energy-band diagram of the materials involved in PSCs

Photovoltaic properties

Photovoltaic properties of three polymers were investigated in BHJ solar cells with the conventional device configuration of glass/ITO/PEDOT:PSS/polymer:$PC_{71}BM$/Ca/Al. The blend ratios (*w/w*) of polymer and $PC_{71}BM$ were changed from 1:1 to 1:3. For all polymers, devices with a D:A weight ratio of 1:1 showed the best performance of 3.0%, 3.6% and 4.2% for PTBFBT-0F, PTBFBT-1F and PTBFBT-2F, respectively. Fig.5 shows the typical *J-V* curves, measured under AM 1.5, 100 $mW \cdot cm^{-2}$. The representative characteristics of the solar cells are summarized in Table 3. The stepwise increase in *FF* was observed with the increasing of fluorine number. The insertion of one fluorine atom on the BT moiety causes the *FF* to increase by 7.5% to 46%. Upon introduction of the second fluorine atom, the *FF* got further improved by 16.2% to 53% for PTBFBT-2F. It was probably due to the noncovalent attractive interactions between S (in thiophene) and F, and between C-H (in thiophene) and N (in BT) which minimize the torsional angle (Figure S3). [39] The smaller torsional angle will maximize the planarity of the polymer chain which can result in an efficient charge transport. Noncovalent coulomb interactions have been utilized to increase the planarity and ordering of polymer chains by many groups.[40-42] Besides the *FF*, the V_{oc} got improved for PTBFBT-1F and PTBFBT-2F when compared with PTBFBT-0F due to the lower HOMO level. However, PTBFBT-1F and PTBFBT-2F exhibited a little lower J_{sc} probably due to blue shifted absorption. Nonetheless, it

requires a balance between V_{oc}, FF and J_{sc} to reach optimum efficiencies. Therefore, PTBFBT-0F obtained the lowest PCE resulting from its lowest V_{oc} and FF although of the highest J_{sc}. While PTBFBT-2F-based solar cells showed elevated PCE up to 4.2% due to the large increase in FF. These results indicate that the photovoltaic properties of conjugated polymer can be effectively tuned by fluorination.[18, 43] The correlation between polymers, V_{oc}, J_{sc}, FF, PCE, hole and electron mobilities are shown in Figure S4, related data are summarized in Table 3.

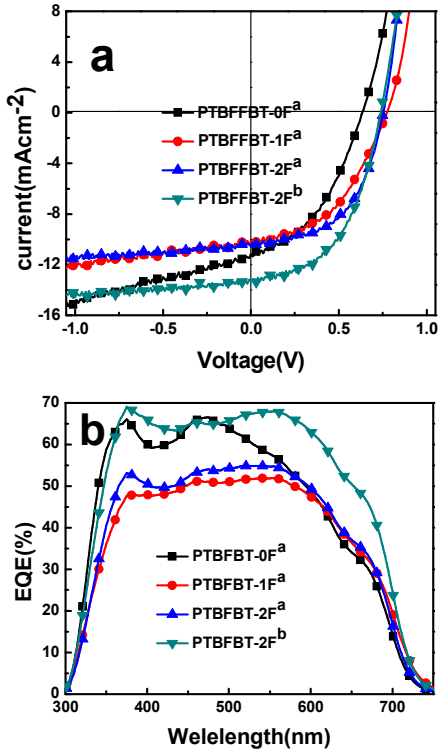

Fig. 5 *J–V* (a) and *EQE* (b) curves of polymer/$PC_{71}BM$-based regular single solar cells under AM 1.5 G illumination, 100 mW cm^{-2}. [a] with Ca, [b] with ZrAcac.

In order to further optimize the device of three polymers, we use ZrAcac as a cathode interlayer between the active layer and Al electrode which induces the increase of J_{sc} values, resulting in a further increase of PCE from 3.0% to 4.1% for PTBFBT-0F, 3.6% to 4.2% for PTBFBT-1F, 4.2% to 5.0% for PTBFBT-2F. All the J_{sc} were in good agreement with the EQE spectra (shown in Fig.5) within an experimental error of 8%.

Charge transport

In order to quantify charge mobilities, hole-only device (ITO/PEDOT:PSS/polymer:$PC_{71}BM$/Au) and electron-only device (Al/polymer:$PC_{71}BM$/Al) were prepared using optimized BHJ films and their *J-V* characteristics were analyzed by the space charge limited current (SCLC) method. The hole and electron mobilities are calculated by Poole-Frenkel Law.[44] Herein, J is current density, d stands for the thickness of the device, and $V = V_{appl} - V_{bi}$, where V_{appl} is the applied potential and V_{bi} is the built-in potential. SCLC model can be described by the equation:

$$J_{SCLC} = \frac{9}{8}\varepsilon_o\varepsilon_r\mu_o\frac{(V-V_{bi})^2}{d^3}\exp[0.89\gamma\sqrt{\frac{V-V_{bi}}{d}}]$$

The results are plotted as $\ln(Jd^3/V^2)$ *vs* $(V/d)^{0.5}$ shown in Fig.6. The hole and electron mobilities of PTBFBT-0F, PTBFBT-1F, PTBFBT-2F were calculated to be 2.65×10^{-6} $cm^2\cdot v^{-1}\cdot s^{-1}$ and 2.25×10^{-5} $cm^2\cdot v^{-1}\cdot s^{-1}$, 1.79×10^{-6} $cm^2\cdot v^{-1}\cdot s^{-1}$ and 7.15×10^{-7} $cm^2\cdot v^{-1}\cdot s^{-1}$, 1.52×10^{-5} $cm^2\cdot v^{-1}\cdot s^{-1}$ and 1.83×10^{-5} $cm^2\cdot v^{-1}\cdot s^{-1}$, respectively. The relatively higher and balanced charge transport of PTBFBT-2F leads to a high FF up to 53%.[45]

Table 3 Device parameters of polymer/$PC_{71}BM$-based PSCs.

Active layer polymer:$PC_{71}BM$ =1:1	CBL	V_{oc} (V)	J_{sc} (mA·cm^{-2})	PCE (%)	*FF* (%)	hole mobilities (cm^2·v^{-1}·s^{-1})	electron mobilities (cm^2·v^{-1}·s^{-1})
PTBFBT-0F	Ca	0.63	11.18	3.0	42	2.65×10^{-6}	2.25×10^{-5}
PTBFBT-0F	Zracac	0.65	12.37	4.1	49		
PTBFBT-1F	Ca	0.77	10.28	3.6	46	1.79×10^{-6}	7.15×10^{-7}
PTBFBT-1F	Zracac	0.77	10.76	4.2	50		
PTBFBT-2F	Ca	0.75	10.54	4.2	53	1.52×10^{-5}	1.83×10^{-5}
PTBFBT-2F	Zracac	0.74	13.32	5.0	50		

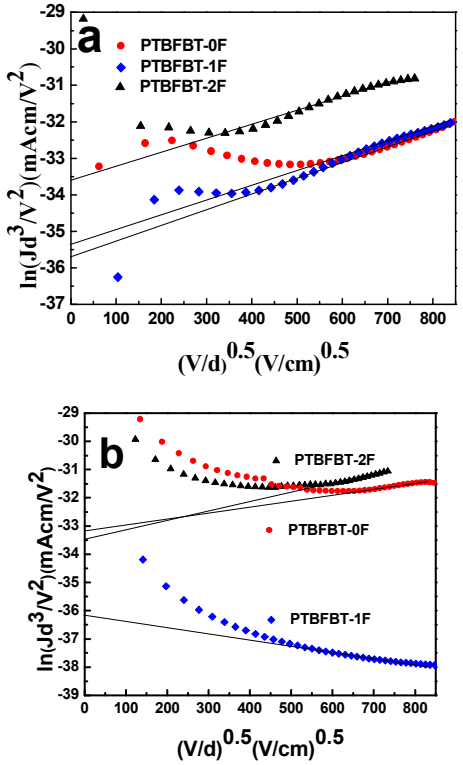

Fig.6 $\ln(Jd^3/V^2)$–$(V/d)^{0.5}$ plots for the polymer:$PC_{71}BM$(1:1, *w*/*w*) based hole-only device (a) and electron-only device (b).

Morphology analysis

Morphology of the BHJ layer is very important for device performance. Donor plays a major role in light absorption and excitons generation. Acceptor splits the excitons and creates electron pathways. Ideally, donors and acceptors would form two distinct continuous phases where the average size of the domains will be tens of nanometers in size.[46]

We investigated the morphologies of polymer and $PC_{71}BM$ blends spin-coated from their *o*-DCB solutions using AFM. Surface topography and phase images were taken for each film and are shown in Figure S5. Root-mean-square (RMS) roughness increases from 0.66 nm for the non-fluorinated case, 1.05 nm for mono-fluorinated to 1.88 nm for di-fluorinated.[47] The nanoscale morphology of blends of three polymers with $PC_{71}BM$ showed bicontinuous networks and are quite similar with only small variations of the RMS.

Another powerful technique is transmission electron microscopy (TEM). The specific density difference of polymer and PCBM enables the polymer-rich and fullerene-rich regions to be mapped. In the PTBFBT-0F/$PC_{71}BM$ blend film images (Fig. 7a), the brighter areas are attributed to the polymer-rich regions, here interconnected via a network of PCBM-rich boundaries.[48] The

slightly coarse phase-separated morphology, compared with PTBFBT-2F/$PC_{71}BM$ blend film, is likely to limit the efficiency of exciton diffusion to the polymer-PCBM interfaces.[49, 50] However, it could be observed that the PTBFBT-2F/$PC_{71}BM$ exhibits moderate homogeneity and there were no detrimental phase segregation and the good miscibility with $PC_{71}BM$ which can explain the excellent *FF* (Fig.7c).

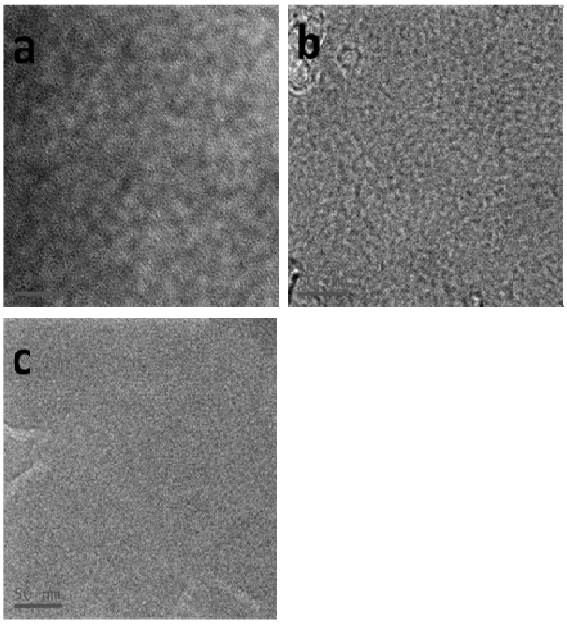

Fig.7 TEM images of PTBFBT-0F/$PC_{71}BM$ film(a), PTBFBT-1F/$PC_{71}BM$ film(b), PTBFBT-2F/$PC_{71}BM$ film(c).

Conclusion

In summary, we have synthesized three copolymers from electron-deficient BT with different fluorine number as acceptor unit and TBF as donor unit, named PTBFBT-0F, PTBFBT-1F and PTBFBT-2F. These polymers were thoroughly investigated. All these polymers display good solution-processed property, sufficient thermal stability and low bandgap. A decrease in the HOMO level and slightly blue-shift absorption of the fluorinated polymer relative to the non-fluorinated polymer were observed. PTBFBT-1F and PTBFBT-2F have similar performance in photophysics and photovoltaic properties except for *FF*. The relatively high and balanced hole and electron transport mobility, bicontinuous and homogeneous morphology led to a high *FF* of PTBFBT-2F. Preliminary photovoltaic cells based on PTBFBT-0F, PTBFBT-1F, PTBFBT-2F as the donor showed the increasing efficiency of 3.0%, 3.6%, 4.2%, respectively. Furthermore, 5.0% efficiency with PTBFBT-2F as the donor was obtained when using ZrAcac as CBL. Therefore, introducing different fluorine number onto the acceptor units in D–A polymers will be a promising method to effectively tune their photophysics and photovoltaic properties.

Acknowledgments

This work was supported by NSFC (Nos. 51173206, 21161160443). The authors acknowledge the NMR measurements from the Modern Analysis and Testing Center of CSU.

Notes and references

R.Cui and L.Fan contributed to this work equally.

[a]*College of Chemistry and Chemical Engineering, Central South University, Changsha, 410083, China E-mail: yingpingzou@csu.edu.cn(Y.Zou)*

[b]*School of Civil Engineering and Mechanics, Xiangtan University, Xiangtan 411105, China*

[c]*College of Chemistry, Xiangtan University, Xiangtan, 411105,*

China

[d]*Beijing National Laboratory for Molecular Sciences, Institute of Chemistry, Chinese Academy of Sciences, Beijing 100190, China*

Electronic Supplementary Information (ESI) available: : Figure S1 giving HNMR spectra of the polymers, Figure S2 giving of X-ray diffraction patterns of three polymers, Figure S3 giving noncovalent attractive interactions within the polymer chain. Figure S4 giving AFM images (3μm×3μm).

1. G. Yu, J. Gao, J. Hummelen, F. Wudl and A. Heeger, *Science-AAAS-Weekly Paper Edition*, 1995, **270**, 1789-1790.
2. C. C. Chen, W. H. Chang, K. Yoshimura, K. Ohya, J. You, J. Gao, Z. Hong and Y. Yang, *Adv Mater*, 2014, **26**, 5670-5677.
3. C. C. Chen, W. H. Chang, K. Yoshimura, K. Ohya, J. B. You, J. Gao, Z. R. Hong and Y. Yang, *Adv Mater*, 2014, **26**, 5670-5677.
4. J. B. You, L. T. Dou, K. Yoshimura, T. Kato, K. Ohya, T. Moriarty, K. Emery, C. C. Chen, J. Gao, G. Li and Y. Yang, *Nat Commun*, 2013, **4**.
5. J. B. You, C. C. Chen, Z. R. Hong, K. Yoshimura, K. Ohya, R. Xu, S. L. Ye, J. Gao, G. Li and Y. Yang, *Adv Mater*, 2013, **25**, 3973-3978.
6. Y. Liu, J. Zhao, Z. Li, C. Mu, W. Ma, H. Hu, K. Jiang, H. Lin, H. Ade and H. Yan, *Nat Commun*, 2014, **5**.
7. W. W. Li, A. Furlan, K. H. Hendriks, M. M. Wienk and R. A. J. Janssen, *J Am Chem Soc*, 2013, **135**, 5529-5532.
8. S. Schumann, R. Da Campo, B. Illy, A. C. Cruickshank, M. A. McLachlan, M. P. Ryan, D. J. Riley, D. W. McComb and T. S. Jones, *J Mater Chem*, 2011, **21**, 2381-2386.
9. V. Kumar, H. M. Wang and C. Rodenburg, *Org Electron*, 2014, **15**, 2059-2067.
10. K. Zhang, C. M. Zhong, S. J. Liu, C. Mu, Z. K. Li, H. Yan, F. Huang and Y. Cao, *Acs Appl Mater Inter*, 2014, **6**, 10429-10435.
11. J. W. Shim, C. Fuentes-Hernandez, Y. H. Zhou, A. Dindar, T. M. Khan, A. J. Giordano, H. Cheun, M. Yun, S. R. Marder and B. Kippelen, *Adv Energy Mater*, 2014, **4**.
12. A. B. Yusoff, S. J. Lee, J. Kim, F. K. Shneider, W. J. da Silva and J. Jang, *Acs Appl Mater Inter*, 2014, **6**, 13079-13087.
13. C. Kitamura, S. Tanaka and Y. Yamashita, *Chem Mater*, 1996, **8**, 570-578.
14. A. C. Stuart, J. R. Tumbleston, H. X. Zhou, W. T. Li, S. B. Liu, H. Ade and W. You, *J Am Chem Soc*, 2013, **135**, 1806-1815.
15. T. Okamoto, K. Nakahara, A. Saeki, S. Seki, J. H. Oh, H. B. Akkerman, Z. Bao and Y. Matsuo, *Chem Mater*, 2011, **23**, 1646-1649.
16. J. W. Jo, J. W. Jung, H.-W. Wang, P. Kim, T. P. Russell and W. H. Jo, *Chem Mater*, 2014, **26**, 4214-4220.
17. H. J. Son, W. Wang, T. Xu, Y. Y. Liang, Y. E. Wu, G. Li and L. P. Yu, *J Am Chem Soc*, 2011, **133**, 1885-1894.
18. M. Zhang, X. Guo, S. Zhang and J. Hou, *Adv Mater*, 2014, **26**, 1118-1123.
19. B. Carsten, J. M. Szarko, H. J. Son, W. Wang, L. Y. Lu, F. He, B. S. Rolczynski, S. J. Lou, L. X. Chen and L. P. Yu, *J Am Chem Soc*, 2011, **133**, 20468-20475.
20. B. S. Rolczynski, J. M. Szarko, H. J. Son, Y. Y. Liang, L. P. Yu and L. X. Chen, *J Am Chem Soc*, 2012, **134**, 4142-4152.
21. H. Zhou, L. Yang, A. C. Stuart, S. C. Price, S. Liu and W. You, *Angewandte Chemie*, 2011, **50**, 2995-2998.
22. H. Bronstein, J. M. Frost, A. Hadipour, Y. Kim, C. B. Nielsen, R. S. Ashraf, B. P. Rand, S. Watkins and I. McCulloch, *Chem Mater*, 2013, **25**, 277-285.
23. B. C. Schroeder, Z. Huang, R. S. Ashraf, J. Smith, P. D'Angelo, S. E. Watkins, T. D. Anthopoulos, J. R. Durrant and I. McCulloch, *Adv Funct Mater*, 2012, **22**, 1663-1670.
24. Y. Zhang, S. C. Chien, K. S. Chen, H. L. Yip, Y. Sun, J. A. Davies, F. C. Chen and A. K. Jen, *Chem Commun (Camb)*, 2011, **47**, 11026-11028.
25. B. Liu, Y. Zou, S. Ye, Y. He and K. Zhou, *RSC Advances*, 2011, **1**, 424-428.
26. L. Xiao, B. Liu, X. Chen, Y. Li, W. Tang and Y. Zou, *RSC Advances*, 2013, **3**, 11869.
27. L. Fan, R. Cui, X. Guo, D. Qian, B. Qiu, J. Yuan, Y. Li, W. Huang, J. Yang, W. Liu, X. Xu, L. Li and Y. Zou, *Journal of Materials Chemistry C*, 2014, **2**, 5651.
28. Y. Huang, X. Guo, F. Liu, L. Huo, Y. Chen, T. P. Russell, C. C. Han, Y. Li and J. Hou, *Adv Mater*, 2012, **24**, 3383-3389.
29. G. Li, C. W. Chu, V. Shrotriya, J. Huang and Y. Yang, *Appl Phys Lett*, 2006, **88**, 253503.
30. H.-H. Liao, L.-M. Chen, Z. Xu, G. Li and Y. Yang, *Appl Phys Lett*, 2008, **92**, 173303.
31. M. Lv, S. Li, J. J. Jasieniak, J. Hou, J. Zhu, Z. Tan, S. E. Watkins, Y. Li and X. Chen, *Adv Mater*, 2013, **25**, 6889-6894.
32. Z.-G. Zhang, B. Qi, Z. Jin, D. Chi, Z. Qi, Y. Li and J. Wang, *Energ Environ Sci*, 2014, **7**, 1966.
33. Z. Tan, S. Li, F. Wang, D. Qian, J. Lin, J. Hou and Y. Li, *Sci Rep*, 2014, **4**, 4691.
34. S. Cho, J. H. Seo, S. H. Park, S. Beaupre, M. Leclerc and A. J. Heeger, *Adv Mater*, 2010, **22**, 1253-1257.
35. Y. Sakamoto, S. Komatsu and T. Suzuki, *J Am Chem Soc*, 2001, **123**, 4643-4644.
36. J. Kim, M. H. Yun, G.-H. Kim, J. Lee, S. M. Lee, S.-J. Ko, Y. Kim, G. K. Dutta, M. Moon and S. Y. Park, *Acs Appl Mater Inter*, 2014, **6**, 7523-7534.
37. B. Liu, X. Chen, Y. Zou, Y. He, L. Xiao, X. Xu, L. Li and Y. Li, *Polym Chem-Uk*, 2013, **4**, 470-476.
38. A. Iyer, J. Bjorgaard, T. Anderson and M. E. Köse, *Macromolecules*, 2012, **45**, 6380-6389.
39. T. L. Nguyen, H. Choi, S. J. Ko, M. A. Uddin, B. Walker, S. Yum, J. E. Jeong, M. H. Yun, T. J. Shin, S. Hwang, J. Y. Kim and H. Y. Woo, *Energ Environ Sci*, 2014, **7**, 3040.
40. Y. F. Wang, S. R. Parkin, J. Gierschner and M. D. Watson, *Org Lett*, 2008, **10**, 3307-3310.
41. X. Guo, J. Quinn, Z. Chen, H. Usta, Y. Zheng, Y. Xia, J. W. Hennek, R. P. Ortiz, T. J. Marks and A. Facchetti, *J Am Chem Soc*, 2013, **135**, 1986-1996.
42. X. G. Guo, F. S. Kim, S. A. Jenekhe and M. D. Watson, *J Am Chem Soc*, 2009, **131**, 7206-+.
43. L. Yang, J. R. Tumbleston, H. Zhou, H. Ade and W. You, *Energ Environ Sci*, 2013, **6**, 316.
44. W. Pasveer, J. Cottaar, C. Tanase, R. Coehoorn, P. Bobbert, P. Blom, D. De Leeuw and M. Michels, *Phys Rev Lett*, 2005, **94**, 206601.
45. Y. Lin, J. Wang, S. Dai, Y. Li, D. Zhu and X. Zhan, *Adv Energy Mater*, 2014, **4**, n/a-n/a.
46. F. Liu, Y. Gu, J. W. Jung, W. H. Jo and T. P. Russell, *Journal of Polymer Science Part B: Polymer Physics*, 2012, **50**, 1018-1044.
47. W. Wang, W. Xu, L. Cosimbescu, D. Choi, L. Li and Z. Yang, *Chem Commun (Camb)*, 2012, **48**, 6669-6671.
48. J. Warnan, A. El Labban, C. Cabanetos, E. T. Hoke, P. K. Shukla, C. Risko, J.-L. Brédas, M. D. McGehee and P. M. Beaujuge, *Chem Mater*, 2014, **26**, 2299-2306.
49. B. A. Collins, Z. Li, J. R. Tumbleston, E. Gann, C. R. McNeill and H. Ade, *Adv Energy Mater*, 2013, **3**, 65-74.
50. S. J. Lou, J. M. Szarko, T. Xu, L. Yu, T. J. Marks and L. X. Chen, *J Am Chem Soc*, 2011, **133**, 20661-20663.

